Chapter 1

Context

1.1 The LHC project

The Large Hadron Collider (LHC) project is CERN's move towards the accelerators of the next generation and is a natural successor to previous particle accelerators. There is little sense in talking about an accelerator without some indication of the physics that is accessible using it and there is not much point in talking physics without being able to measure anything ... without having a detector in the case of an accelerator.

1.1.1 Historical motivation

The first ideas for the LHC appeared in the early 1980's. These were the times after the discovery of the W and Z bosons by the UA1 and UA2 collaborations at CERN which gave new wind to physicists sailing the sea of the Standard Model. The large electron-positron collider (LEP) was being built together with the four experiments that were to become the messengers of its glory. LEP was seen as the machine to provide high precision measurements of the Standard Model in the electro-weak sector.

A major problem with the electron accelerators is the huge energy loss due to synchrotron radiation (proportional to γ^4) which makes them true energy suckers also during continuous beam operation. An alternative obvious choice is to use proton–antiproton collider ... but at high energies the collisions are between partons and therefore we only use some fraction of proton's energy in a single reaction. Going up in energy hits back with the cross-section dependency on the cms energy which is roughly proportional to $1/Q^2$ so one must also increase the luminosity. By going to a higher luminosity one encounters two problems. The first is that one needs high incoming currents of particles and massive production of anti-protons is technologically difficult. It is more reasonable to make two parallel beam-pipes with specially designed dipole magnets. The second problem is that the high density of charged particles in a bunch makes it a nightmare to keep them together without significant losses.

Nevertheless, it was already obvious that machines with a higher energy and higher luminosity would be needed to make one step further ... to get to the gist of spontaneous symmetry breaking (the Higgs boson hunt) and to produce b and t quarks in the abundance needed for spectroscopy. Super-symmetric and string theories were lurking in the theoretical mist pointing to energies in the TeV region. In astrophysics dark matter was haunting the souls seeking their comfort in the cosmological models giving rise to ideas of new states of matter (like lepto-quarks, excited leptons and quark-gluon plasma). Fermilab was building the Tevatron proton–antiproton collider and plans for the SSC were slowly emerging. All of these things were putting imagination on fire and in 1990 there was a LHC Workshop held at Aachen organized by the European Committee for Future Accelerators [1]. The basic building blocks of the project were presented: physics for different modes of LHC operation, the basic parameters of detectors that could be used in the LHC environment and data acquisition services needed (electronics and software tools). In 1992 the LHC committee was established at CERN and in 1993 'Letters of Intent' to build a detector at the LHC were submitted by the ALICE, ATLAS and CMS collaborations followed by the LHC–b collaboration in 1994.

1.1.2 Technical details

The primary operation of the LHC will be in *pp* collisions at 14 TeV cms energy with a luminosity starting at $\sim 3 \cdot 10^{33}$ in the first year, increasing to $\sim 10^{34}\,\mathrm{cm}^{-2}\,\mathrm{s}^{-1}$ for the rest of the operation. Studies of heavy ion collisions with Pb-Pb beams accelerated up to 1250 TeV (2.76 TeV/u) are also planned. As main physics goals of the ATLAS and cms collaborations require the *p-p* mode, all numbers will be quoted for this regime.

The LHC will be filled from the Super Proton Synchrotron (SPS) with 450 GeV bunches consisting of 1.1×10^{11} protons (see Fig.1.1 for a schematic view). Acceleration to 7 TeV will take 4.3 minutes during which the magnetic field in the dipole bending magnets will increase from 0.535 T to 8.33 T. Luminosity is designed to be maintained at a usable level for 10 hours. The energy loss via synchrotron radiation will be 3.8 kW which poses a technical difficulty for cryogenics (the beam-pipe, the RF cavities and the bending magnets will be held at a temperature of 1.4 K). The bunch spacing will be 7.48 m (or 24.95 ns). A single bunch will have a length of 8.4 cm (or 0.28 ns) and a fractional energy spread of $0.105 \cdot 10^{-3}$.

1.2 Life cycle of an HEP experiment and the importance of beam tests

In high energy physics one deals with particles of various energies, lifetimes, decay modes and the properties of interaction with matter. From a theoretical point of view one attempts to understand the interaction process in terms of a physical model. But to 'see' the process one needs to detect the final state particles and to perform some sort of measurement in order to assign them momentum and energy as well as to identify them.

When a new HEP experiment is being planned, the physical goals are set first. The beam particle-type and energy are usually known in advance, so the production mechanisms and final-state kinematics for the processes of interest can be established. The sought-for precision of measurements is the first source of requirements for the precision of the detector. For each candidate channel, a similar reasoning is followed to identify the processes that result in the same (or at least indistinguishable) signature in the detector as the studied process; these processes are called *background*. Here extreme caution is paid to assure a statistically significant signal over background ratio, since the production cross-sections of the background processes can be orders of magnitude above the cross-section for the process of interest. From the required background rejection factors, the second set of requirements for the detector precision is determined. Based on the requirements and available resources,

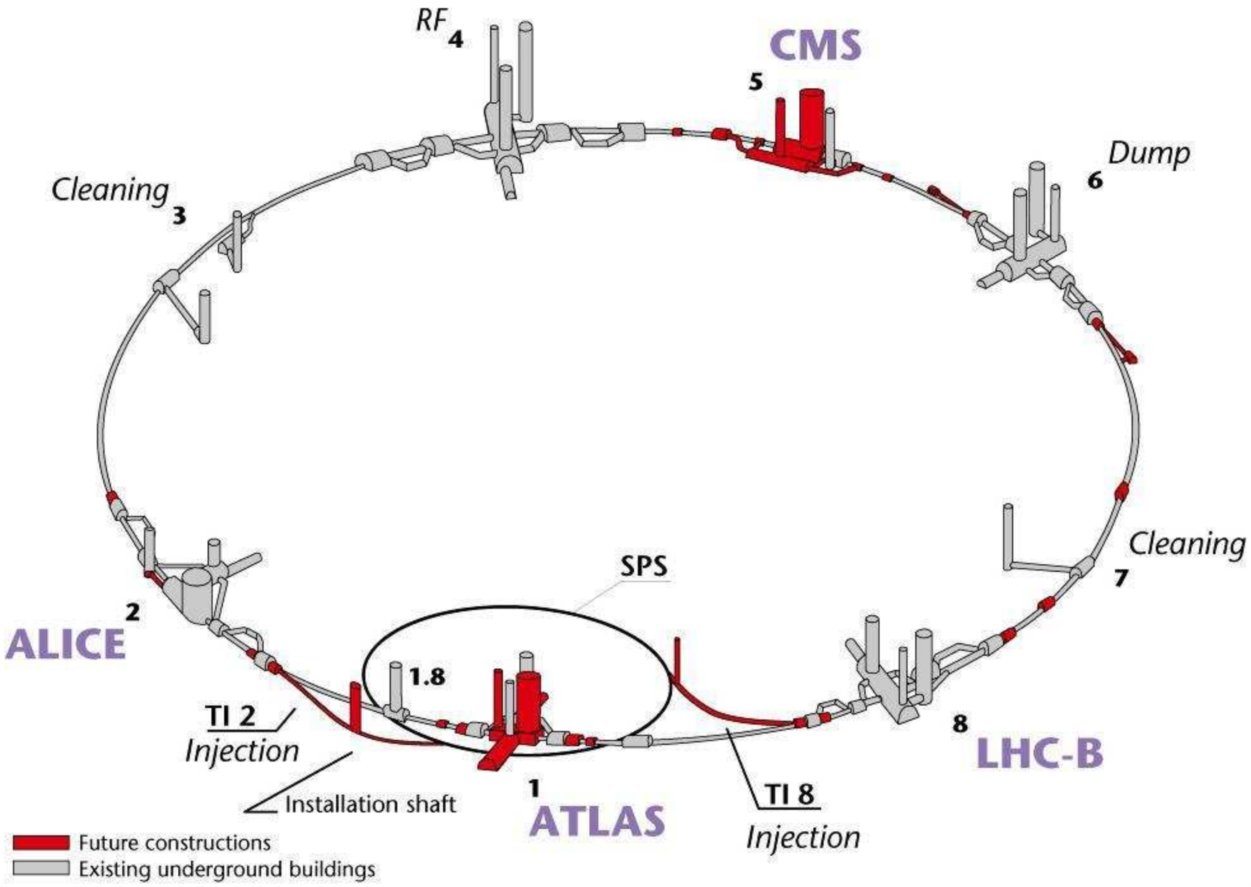

Figure 1.1: Schematic view of the LHC accelerator.

the detector elements are chosen. Furthermore, the sub-detector specifications are deduced from the detector physics requirements.

As HEP experiments probe deep into the quantum structure of nature, the interaction of particles with a sensitive material is of probabilistic nature (or statistical if one prefers this formulation). The detectors used are often constrained by a large number of requirements, some of them entirely earthly in origin (cost is one of the most painful ones), which makes the optimisation of a given detector a delicate process. That's why we need to put the detectors at different stages of development into a test beam: to see the detector and related electronic response in a near real-life situation. Results help us evaluate the device, give us development guidelines and in later stages provide a means for testing prototypes before entering into mass production. Another important use of the beam test data is to provide the detector simulation tools with ample sources of cross-checks and calibrations. Without that we could never be certain that our simulations are really describing the animal we're building.

In a large scale HEP experiment test beam analyses are used during pre-production stage using the prototypes of detector elements. To go into slightly more detail, the evolution of an experiment can be roughly apportioned to four phases taking into account the manpower (in terms of educational structure and quantity) and infrastructure involved.

The early planning phase begins with a handful of people becoming aware of a technical possibility to probe into a more or less uncharted territory of physics. Questions asked are 'Can we do it?' and 'How can we do it?' and the answers are in a somewhat sketchy form. Problems are addressed to a certain depth but not in every possible detail. However the goals are well defined and the areas where surprises or difficulties are expected are pointed out.

The experiment planning phase leads from a 'Letter of Intent' to a 'Technical Proposal'. A detailed study of the main physics being addressed is made from the theoretical point of view and several detector geometries are simulated to find the best solution for a set of often antipodal demands. This is where the base of the experiment's pyramid of scientific force begins to form: institutes (or groups) with previous experience join the experiment to provide solutions for the sub-detectors which are expected to form the detector. Also, estimates are made on requirements for electronics and CPU power.

The experiment preparation and building phase is where everything must be studied down to the smallest detail. Three goals must be satisfied:

- A detailed specification and preparation of the technical support needed by the experiment is required. This includes engineering of the experimental area, services, DAQ systems and computational infrastructure.

- A final choice of detector elements must be made. They must be tested and proven to work in experimental conditions with given requirements from the physics programme and DAQ capabilities. A detailed simulations of the detector's geometry and response is prepared and cross-checked with beam test data obtained from prototypes of sub-detectors.

- Analysis programs must be prepared in order to test the detector acceptance for relevant processes with Monte-Carlo simulations and give feedback to detector engineering.

The results of all this work are presented in the experiment's *Technical Design Report* (TDR). It gives a detailed account of every part of the detector, its performance and its mode of operation.

Experiment building is the actual work of constructing the experiment. In time aspect it largely overlaps with the preparation since decision making and selection process for specifications of subsystems goes from coarse description to fine tuning. This way parts of the system can be built before the final specifications are agreed upon.

The experimental operation begins with data collection. In the commissioning phase the detector's operation is scrutinized and its response optimised in respect to available parameters. Quality assessment is made and calibration of the detectors carried out. Analyses prepared at previous stages are fine tuned to the existing system ... the real physics begins.

1.3 ATLAS experiment and ATLAS detector

The ATLAS collaboration will build a general-purpose pp detector designed to exploit the full discovery potential of the LHC (see ATLAS Physics TDR [2], [3] and ATLAS Technical

Proposal [4]). The major focus of interest for ATLAS is the origin of mass at the electro-weak scale. Detector optimization is therefore guided by physics issues such as the sensitivity to the largest possible Higgs mass range. Other important goals are the searches for the heavy W and Z-like objects, for super-symmetric particles, for compositeness of the fundamental fermions, as well as the investigation of CP violation in B-decays, and detailed studies of the top quark. The ability to cope well with a broad variety of possible physics processes is expected to maximize the detector's potential for the discovery of new, unexpected, physics.

As the LHC physics depends crucially on the high luminosity, it is important to select processes with distinguishable, robust signatures that allow for high-precision measurements and an efficient background rejection. Processes with e and μ leptons as well as photons in the final state are a natural choice in the LHC environment. Furthermore, to allow for a missing transverse energy determination and for a hadronic jet energy measurement, a hermetic hadronic calorimetry is also vital. Since heavy-quark systems will be an important chapter of the LHC physics, a precise secondary vertex determination, full reconstruction of final states with relatively low-p_T particles (e.g., $J/\Psi \to l^+l^-$), low-p_T lepton first level trigger thresholds as well as second-level track triggering capability are all necessary requirements for the experiment. The variety of signatures is considered to be important in the high-rate environment of the LHC in order to achieve robust and redundant physics measurements with the ability of an internal cross-check.

All things considered, one can summarize the basic design considerations for ATLAS in the following points:

- very good electro-magnetic calorimetry for electron and photon identification and measurements, complemented by hermetic jet and missing E_T calorimetry;
- efficient tracking at high luminosity for lepton momentum measurements, for b-quark tagging, and for enhanced electron and photon identification, as well as for τ and heavy-flavour vertexing and a reconstruction capability of some B decay final states at lower luminosity;
- stand-alone, precision, muon momentum measurements up to the highest luminosity, and very low-p_T trigger capability at lower luminosity.

Secondary goals to maximize the physics reach and to optimize the exploration of the LHC give two additional points:

- large acceptance in η coverage;
- triggering and measurements of particles at low-p_T thresholds.

1.3.1 Structure of the detector

The overall detector concept of the ATLAS detector, dictated by the requirements listed above, is not far from the general detector layout of LEP experiments. Going outwards from the interaction point, the first large block one encounters, is the inner detector encompassed by a solenoidal magnetic field and followed by the electro-magnetic and hadronic calorimeters. On the outside of the detector there is the muon system equipped with an air-toroid magnet system for stand-alone momentum measurements. It defines the overall dimensions of the ATLAS detector: outer barrel chambers are at a radius of 11 m and the third layer

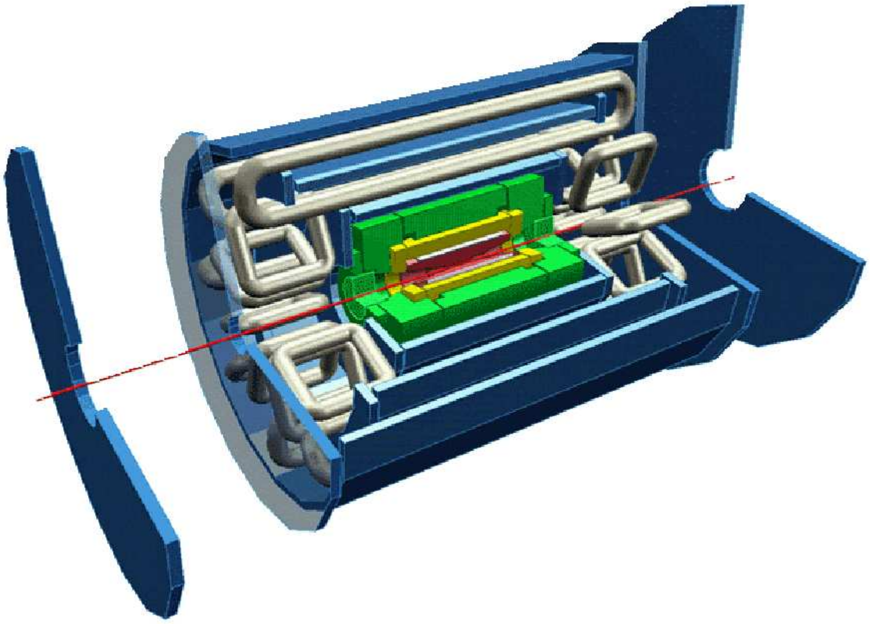

Figure 1.2: A schematic view of the ATLAS detector.

of the forward muon chambers is located ±21 m from the interaction point. Fig:1.2 shows a schematic overview.

1.3.2 Inner detector

The Inner Detector (ID, also called inner tracker) is composed of three parts: the silicon pixel detectors, the silicon strip detectors (*SemiConductor Tracker* – SCT) and the transition radiation tracker (TRT). It combines the high-resolution detectors at inner radii with continuous tracking elements at outer radii. An overview of the inner tracker can be seen in Fig.1.3. Each of the above mentioned sub-detectors has a barrel region (up to $|\eta| \lesssim 1$) where detector layers are arranged on concentric cylinders around the beam axis, while in the forward region (or end-cap) detectors are mounted on disks perpendicular to the beam axis. This can be clearly seen in Fig.1.4 and will be explained in detail together with the separate detector parts. The full ID extends over $|\eta| \leq 2.5$.

The ID is enclosed within a super-conducting solenoid of 5.3 m length (to be compared to the ID's length 6.7 m) creating an axial magnetic field with a strength of 2 T. Since the coil is shorter than the tracking volume the field deviates significantly from uniformity ($B_z \sim 1$ T at the end of the coil and $B_z \sim 0.4$ T at the end of the tracker). This poses some technical difficulties for the pattern recognition algorithms.

The detailed requirements for the ID can be found in [5]:Ch:2.3. They include the geometrical specifications (η coverage, number of space-points per track), the measurement precision (p_T, vertex position), the pattern recognition efficiencies and physics requirements (e/γ identification, secondary vertex resolutions and b-tagging).

The Pixel Detector is designed to provide a very high-granularity, high-precision set of measurements as close to the interaction point as possible. There are three pixel barrels (at radii 47.5 mm, 105.5 mm and 137.5 mm) and four forward disks (with z coordinates

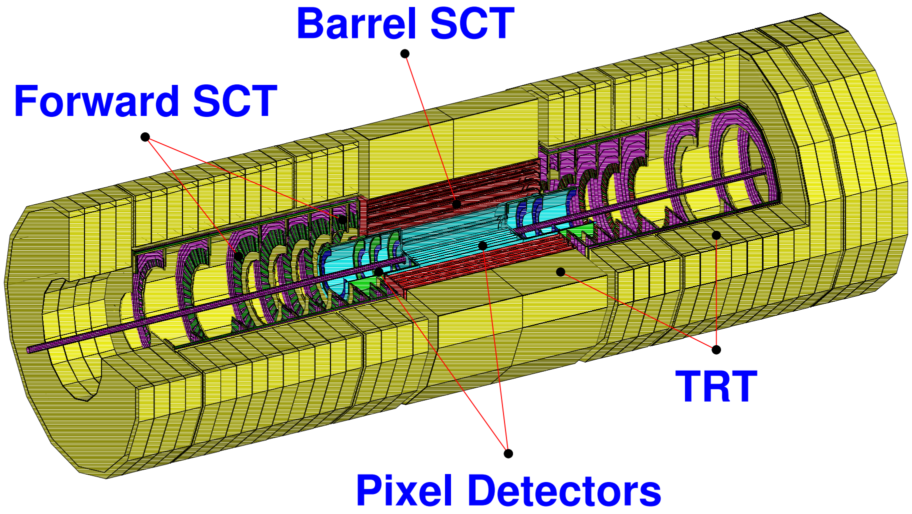

Figure 1.3: A look into the inner tracker.

of 490 mm, 608 mm, 759 mm and 1035 mm), giving at least three measurements of track intersection with a precision of $\delta R\varphi \times \delta z = 50\,\mu m \times 300\,\mu m$.

Its most important role is to provide the desired vertex resolution and enable one to find secondary vertices to be used for the b and τ–tagging. For a complete description see [6].

The Semiconductor Tracker is designed to provide four precision measurements per track in the intermediate radial range, contributing to the measurement of momentum, impact parameter and vertex position, as well as providing good pattern recognition as a result of the detector's high granularity and low occupancy. The barrel SCT has four layers at radii from 30 cm to 52 cm with active half-length of 74.5 cm. The layers are composed of modules consisting of two pairs of silicon micro-strip detectors glued back-to-back with a small stereo angle to obtain the z measurement. Each silicon detector has 768 active readout strips (80 μm pitch) and measures 12.8 cm in length (composed of two 6.4 cm detectors with bonded strips). The end-cap SCT has nine axial wheels positioned at z coordinates from 83.5 cm to 277.8 cm. Forward modules are very similar in design but use tapered strips with one set aligned radially. Technical details of the SCT are presented in [7]:Ch:11.

The TRT is the outermost part of the ID. It consists of 370,000 straws made of coated polyamide film. Their diameter is 4 mm and their length is in the range 40-150 cm (depending on the straw position). In the barrel region straws are parallel to the beam pipe and are mounted on rings. They are embedded in stacks of polypropylene/polyethylene fibre radiator which produces the transition radiation (TR). The end-cap straws are placed radially and regular foils are used for the TR production. Straws are filled with a mixture of 70% Xe + 20% CF_4 + 10%CO_2. Xe allows for detection of the transition radiation (by the use of a double threshold) and contributes significantly to the electron identification power of ATLAS. CF_4 increases the drift velocity and CO_2 is necessary to stabilize the operation. The TRT also contributes to the accuracy of the momentum measurement by providing (on average) 42 measurements in R-φ direction with a resolution of 170 μm per straw. You can also try your luck with [6]:Ch:12.

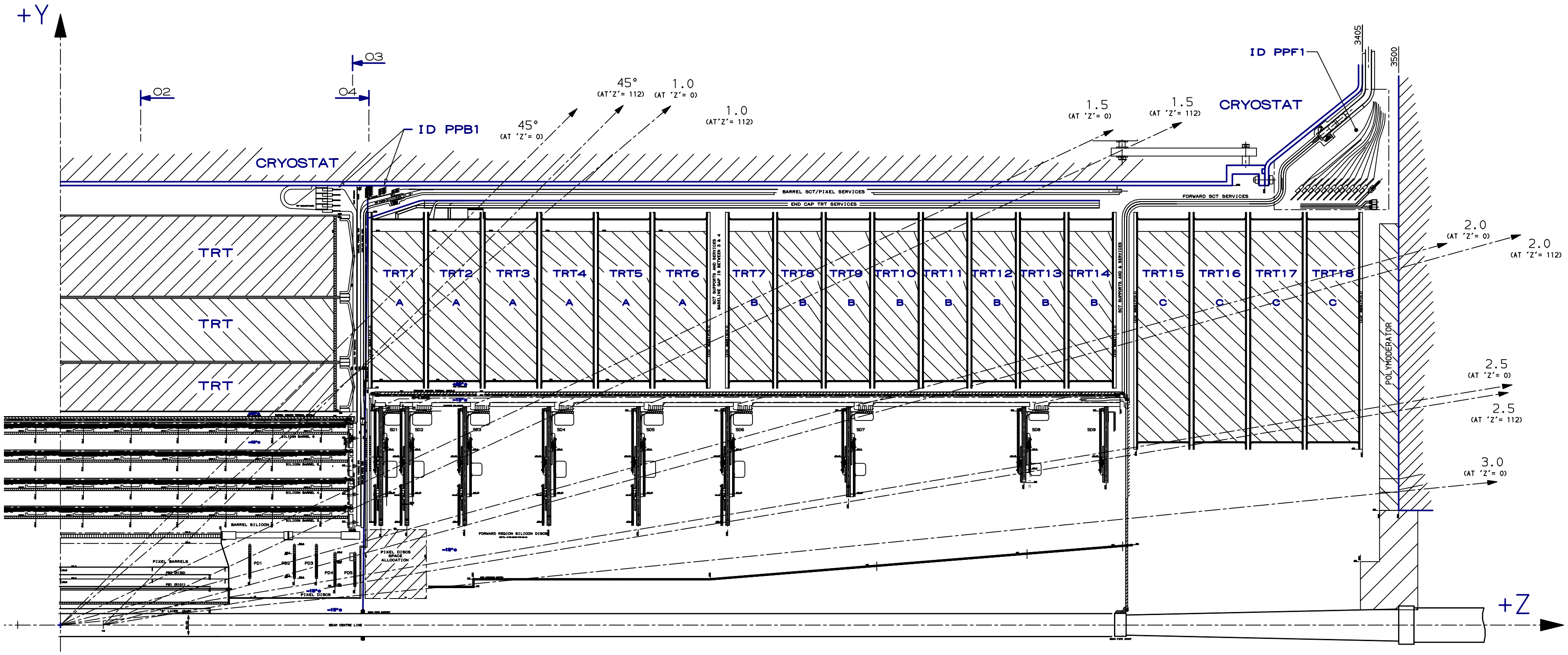

Figure 1.4: An engineering drawing of the ID (a ‘Post TDR’ layout).

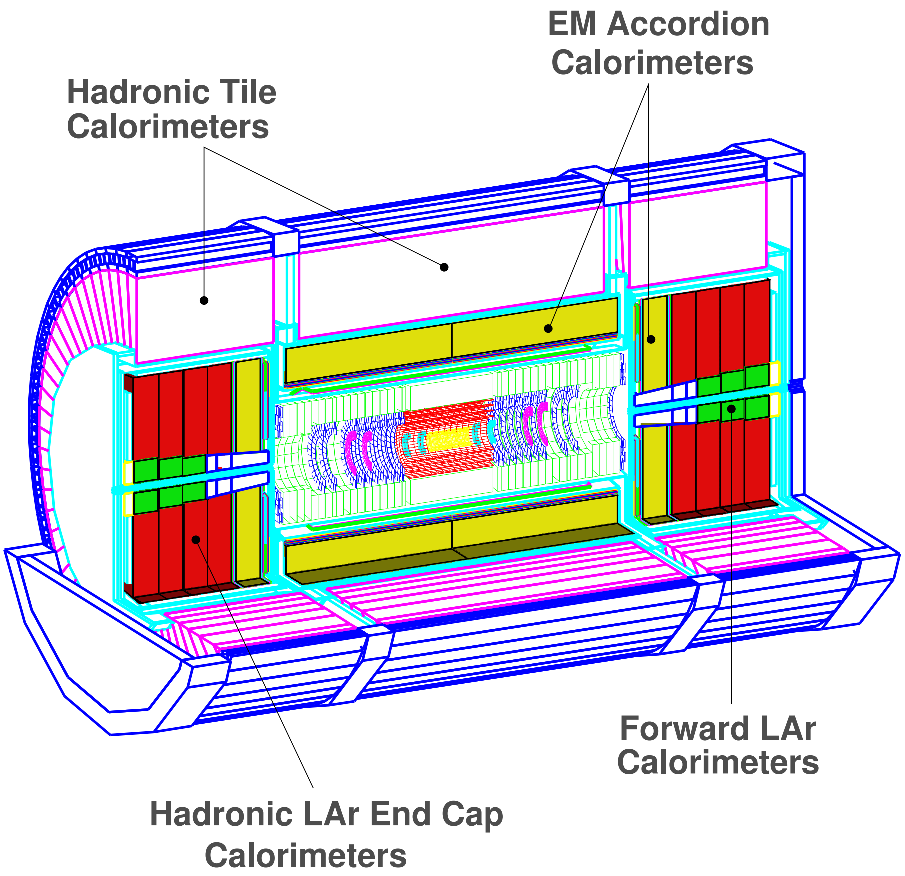

Figure 1.5: Overview of ATLAS calorimetry.

1.3.3 Calorimetry

At the LHC experiments calorimeters are of great importance as their intrinsic resolution improves with energy. The main calorimeter tasks at ATLAS are:

- an accurate measurement of the energy and position of electrons and photons;
- a measurement of the energy and direction of jets;
- a measurement of the missing transverse momentum;
- particle identification;
- event selection at the first trigger level.

The operational environment at the LHC poses several difficulties: the large center-of-mass collision energy implies the need for a good performance over an unprecedented range, extending from $< 1\,\mathrm{GeV}$ up to the TeV scale. At high luminosity a signal from the soft hadronic interactions will be piling-up, both in space and time. A fast detector response and fine granularity are therefore required to minimize its impact on physics performance. The position of the calorimeters in ATLAS is shown in Fig.1.5. A detailed description of the calorimeter's performance is available in [8].

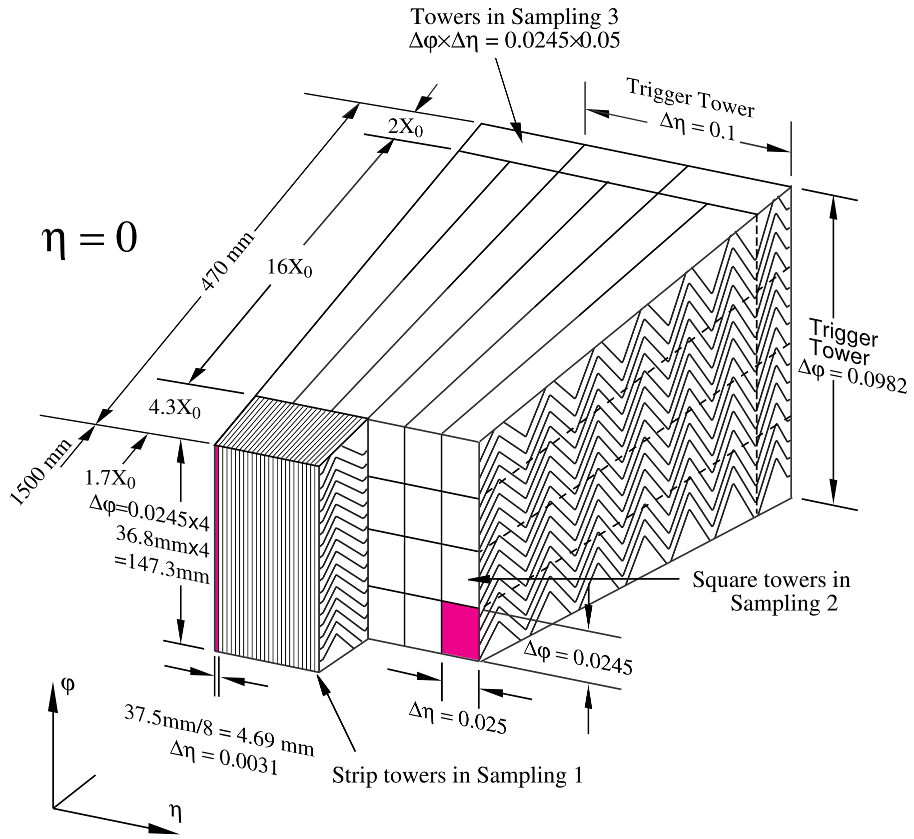

Figure 1.6: A sketch of the structure of the EM calorimeter.

EM calorimeter

The EM calorimeter is a lead-liquid-argon sandwich detector with accordion-shaped kapton electrodes and lead absorber plates over its full coverage. The lead thickness in the absorber plates has been chosen as a function of rapidity, so as to optimise the calorimeter performance in terms of energy resolution. It covers the rapidity region $|\eta| < 3.2$ with total thickness of > 24 radiation lengths (X_0) in the barrel ($|\eta| < 1.475$) and $\sim 26X_0$ in the end-cap ($1.375 < |\eta| < 3.2$). The energy resolution is $\delta E/E \sim 10\%/\sqrt{E(\,\mathrm{GeV})}$ with the constant term smaller than 1%. The linearity of response is better than 0.5% for energies up to 300 GeV. Measurement of shower direction has a resolution of $\sim 50\,\mathrm{mrad}/\sqrt{E(\,\mathrm{GeV})}$.

The EM calorimeter is divided into towers pointing away from the interaction point and has three longitudinal samplings (see Fig.1.6). In the region $|\eta| < 1.8$ a presampler is installed in front of the calorimeter to correct for the energy lost in the upstream material. It is a 1.1 cm thick (5 mm for $|\eta| > 1.5$) active LAr layer with a segmentation $(\Delta\eta \times \Delta\varphi) = (0.0025 \times 0.1)$. The first sampling is $6X_0$ thick (including dead material and presampler) and has a granularity of $(\Delta\eta \times \Delta\varphi) = (0.003 \times 0.1)$. This very high precision in η is needed for $\pi^0 : \gamma$ separation (π^0 decays almost exclusively as $\pi^0 \to \gamma\gamma$). The second sampling has square towers of size $(\Delta\eta \times \Delta\varphi) = (0.025 \times 0.025)$ and thickness of $16X_0$. The third sampling with thickness from 2 (central barrel) to 12 X_0 and a twice coarser granularity in η is reached only at transverse energies above 50 GeVand is also used for the prediction of leakage into the hadronic calorimeter. In the region of transition from the barrel to end-cap there is a crack in the active material ($1.4 < |\eta| < 1.6$). Scintillators are installed there to allow for

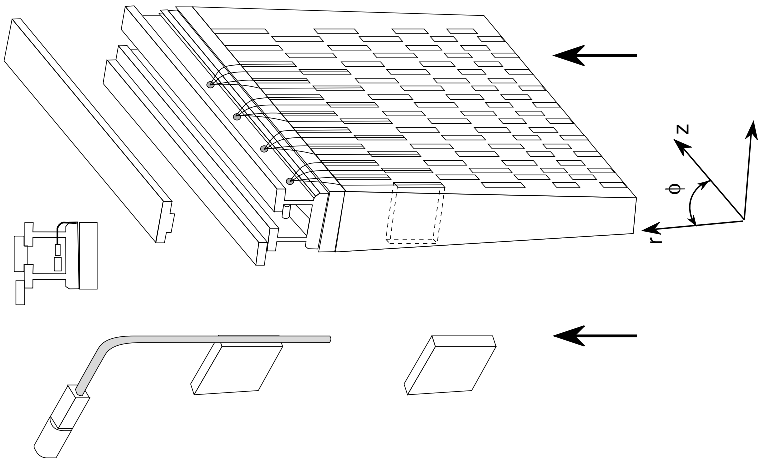

Figure 1.7: A module of the iron tile-scintillator.

the measurement of energy lost in this region. The details of this detector can be found in [9].

Hadronic calorimeter

The ATLAS hadronic calorimetry covers the range $|\eta| < 5$ using different techniques and devices as best suited for the different requirements and radiation environment. The main calorimeter task is the reconstruction of jets and the measurement of missing E_T. The designated energy resolution is $50\%/\sqrt{E} \oplus 3\%$ for $|\eta| < 3$ and $100\%/\sqrt{E} \oplus 10\%$ for $3 < |\eta| < 5$. The linearity of the energy measurement up to 4 TeV is within 2%.

In the barrel region ($|\eta| < 1.5$) iron tile-scintillators are used with an overall thickness of 11 interaction lengths (λ_l) and a granularity of $(\Delta\eta \times \Delta\varphi) = (0.1 \times 0.1)$. The schematic of the tile calorimeter module is shown in Fig.1.7.

In the end-cap and forward regions (see Fig.1.5) a similar technique as in the EM calorimeter (LAr accordion) is used because of the sensitivity of plastic scintillators to radiation damage. Copper is used instead of lead and the plates themselves are some ten times thicker. The granularity in this region is $(\Delta\eta \times \Delta\varphi) = (0.2 \times 0.2)$ and the overall thickness is $14\lambda_l$. For more information consult [10] and [9].

1.3.4 Muon system

High-momentum muons provide a clear and robust signature of physics at the LHC. To exploit this potential, the ATLAS collaboration has designed a high-resolution muon spectrometer with a stand-alone triggering and momentum measurement capability (see [11]).

The spectrometer covers the pseudorapidity range $|\eta| < 2.7$ with divisions into barrel and end-cap regions (Fig:1.8). The magnet system consists of three air-core superconducting toroids. The barrel toroid's length is 25 m with inner and outer bores located at a radius of 9.4 m and 20.1 m respectively. The two end-cap toroids are inserted in the barrel at each end. Their length is 5 m and the bore radii are 1.65 m and 10.7 m. Each toroid consists of eight flat coils assembled radially around the beam axis. Typical bending powers are 3 T m in the barrel and 6 T m in the end-cap.

Over most of the η coverage a precision measurement of the track coordinate in the principle bending plane is provided by three stations of monitored drift tubes (MDT). At large pseudorapidities and close to the interaction point cathode strip chambers (CSC) with higher granularity are used. Their response time is about 500 ns. The resolution of each measurement is 50 μm giving a momentum precision of $\Delta p/p = 10^{-4} \cdot p/[\,\mathrm{GeV}]$ for $p_T >$ 300 GeV. At smaller momenta the resolution is limited to a few percent by multiple scattering in the inner parts of the detector.

The trigger chambers extend up to $|\eta| < 2.4$. Resistive plate chambers (RPC) are used in the barrel and thin gap chambers (TGC) are used in the end-cap region. Both have response times of about 5 ns. They serve for first level triggering, bunch crossing identification and provide measurement of the second coordinate in a direction orthogonal to the one measured in the precision chambers with a typical resolution of 5-10 mm. The p_T acceptance of the muon trigger extends down to $p_T \sim 5$ GeV which is needed for physics studies, including CP violation in the b-quark sector.

1.4 ATLAS Trigger system and computing infrastructure

The collision rate at the LHC will be 40 MHz and the number of binary output channels from the ATLAS detector is approximately 10^7, giving a data-flow of approximately 4×10^{14}bit/s. This is far too much data to be effectively handled and stored. Besides, one doesn't want to study soft hadronic interactions but only the 'interesting' physics at and above the m_W scale, as well as some selected b-hadron events. The luminosity and the estimated pp cross-sections at 14 TeV are expected to yield about 100 such events per second. This gives 100 MB/s of output from the detector, which we believe can be managed by future data storage systems. For comparison, note that LEP experiments produced less than 1 MB/s.

1.4.1 Overview of the ATLAS trigger

The ATLAS trigger is divided into three levels (see Fig.1.9). Each of them performs some specialized functions and the number of events processed by each level becomes progressively smaller.

The Level 1 trigger bases its decisions solely on calorimeter and muon system information. In addition, the granularity used by the Level 1 is coarser than the full detector granularity. It reduces the event rate from 40 MHz to about 10-100 kHz.

The Level 2 trigger uses output from Level 1 to guide it toward the regions of interest (RoI), does unpacking of the ID tracking information and uses the full calorimeter granularity in these regions. By doing track reconstruction it then makes a decision based on the status of allowed trigger menus. This will be discussed in more detail in the following sections. The output rate from Level 2 is 0.1-1 kHz.

Events passing the Level 2 trigger enter the full-reconstruction phase or the Level 3 trigger where the standard offline software is used to build the events. This means using the full detector information and a current version of the reconstruction software. At the end the final decision is made: will the event be stored or not. If so, the event is stored together with the reconstruction information that tags the event with its particle content and can later be

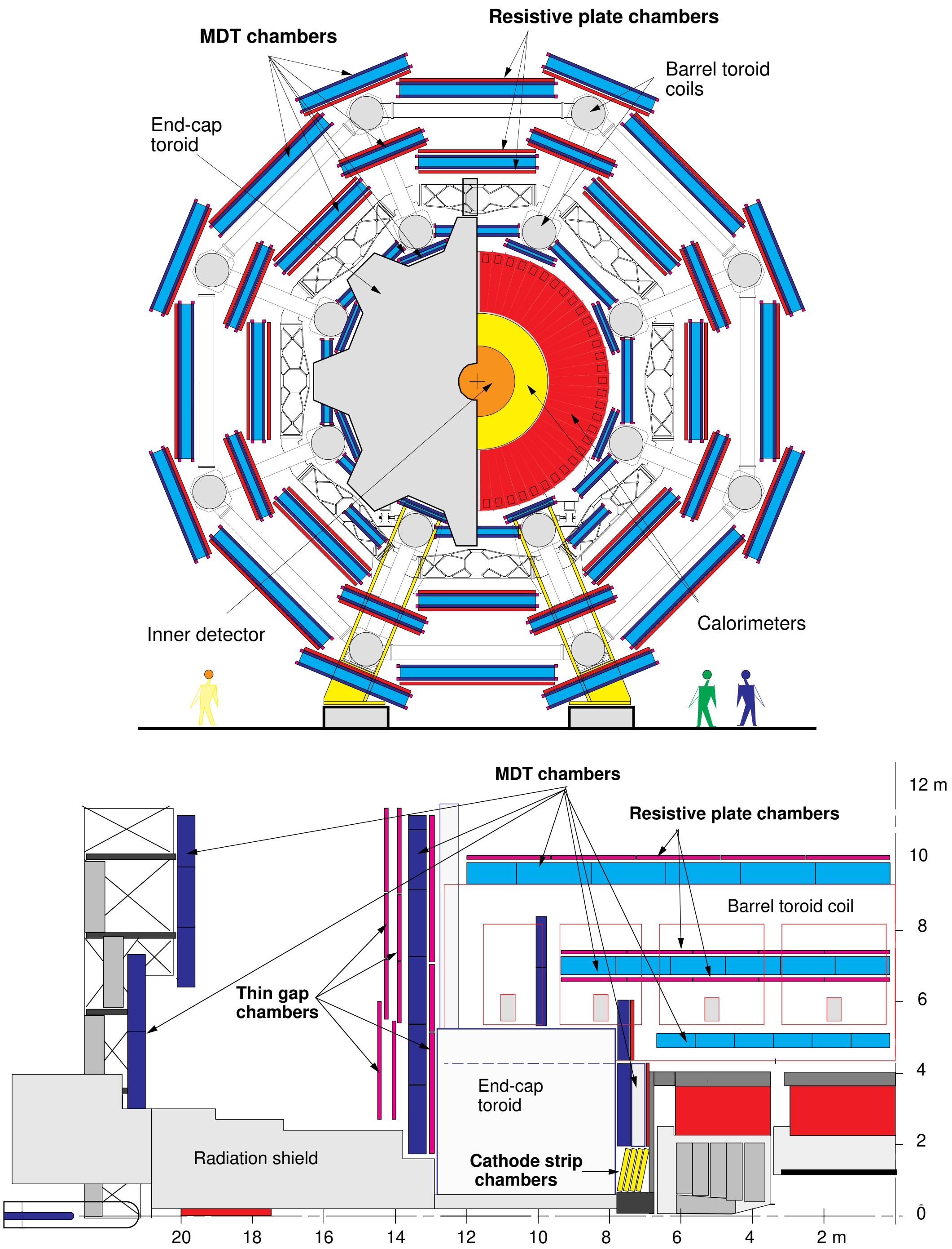

Figure 1.8: x-y (top) and r-φ (bottom) view of the ATLAS muon spectrometer.

used as a selection criteria for detailed analysis. The output rate from Level 3 is the wanted 10-100 Hz.

This last step can later be repeated with a more accurate version of the reconstruction software and new tags can be added to its record but the final selection has already been made.

First of all we have to decide what interests us. Which means that we must write down the physical processes, identify their detectable decay channels and find their signatures in the detector. Then we must study them in the context of the detector and surrounding physics, which will create the background.

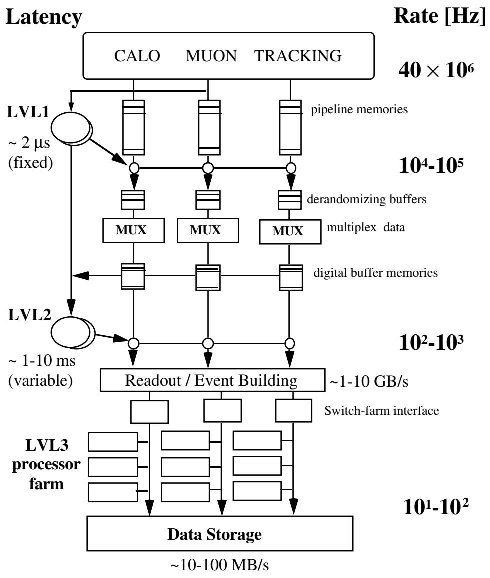

Figure 1.9: Overview of the 3-level ATLAS trigger.

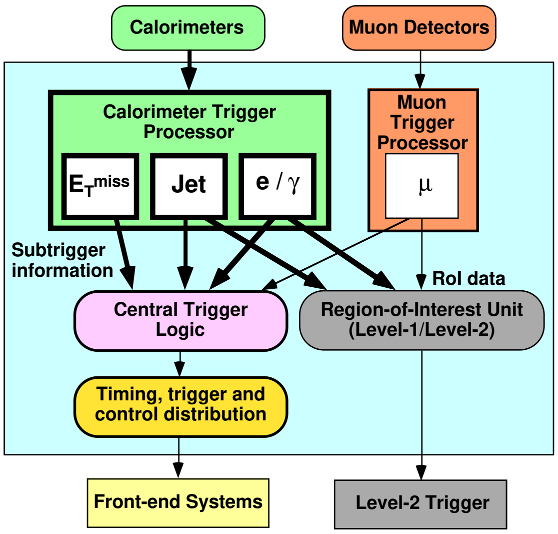

Figure 1.10: An overview of the Level 1 logic.

1.4.2 The Level 1 trigger

As the Level 1 trigger is the most critical part of the system its detailed study is the subject of a dedicated TDR ([12]). Only a brief sketch of its workings is presented here. Level 1 bases its decision on calorimeter and muon system data (see Fig.1.10 for an overview). Custom-made electronics processes the incoming information and generates a list of trigger objects. This list includes:

- information on multiplicity of e, γ above several thresholds
- information on multiplicity of jets above several thresholds
- information on multiplicity of μ above several thresholds

Trigger	Rate [kHz]
Single muon, $p_T > 6\,\mathrm{GeV}$	23
Single isolated EM cluster, $E_T > 20\,\mathrm{GeV}$	11
Two isolated EM clusters, $E_T > 15\,\mathrm{GeV}$	2
Single jet, $E_T > 180\,\mathrm{GeV}$	0.2
Three jets, $E_T > 75\,\mathrm{GeV}$	0.2
Four jets, $E_T > 55\,\mathrm{GeV}$	0.2
Jet, $E_T > 50\,\mathrm{GeV} \oplus$ missing $E_T > 50\,\mathrm{GeV}$	0.4
Tau, $E_T > 20\,\mathrm{GeV} \oplus$ missing $E_T > 30\,\mathrm{GeV}$	2
Other triggers	5
Total	~ 40

Table 1.1: An example of the Level 1 trigger objects and their expected rates for the low luminosity operation.

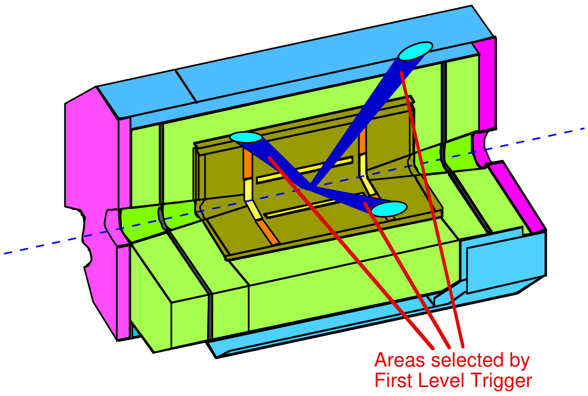

Figure 1.11: The typical regions of interest generated by the Level 1.5 trigger.

- information on $\not{E}_T$.

This list is then compared to the current Level 1 menu. An example of a Level 1 menu is shown in Tab:1.1. These are inclusive objects ... an event can match more than one of them. When we have a match, the event is passed to an intermediate step (Level 1.5 trigger) to build RoIs for Level 2 (Fig.1.11). As you might expect, the RoI builder must be fully aware of the structure of the Level 2 menus in order to feed it with the appropriate search regions.

The processing time (or latency) is fixed to $2.5\,\mu$s and the input flow of data is 1500 Gbit/ s. Until now, read-out has been done only on some detector parts and only if the event passes the Level 1, will the full detector data be read out. This means that each piece of the detector (e.g., an SCT module or EM calorimeter block) must hold the results of the last $2.5\,\mu$s (last 100 events) stored in a pipeline in case the Level 2 trigger will request the full information to be available for any event.

1.4.3 The Level 2 trigger

As an event passes to Level 2 (Fig.1.12) the read out buffers (ROB) are filled from the detector. The input flow is 150 Gbit/ s. From the ROBs each RoI's data is sent over the

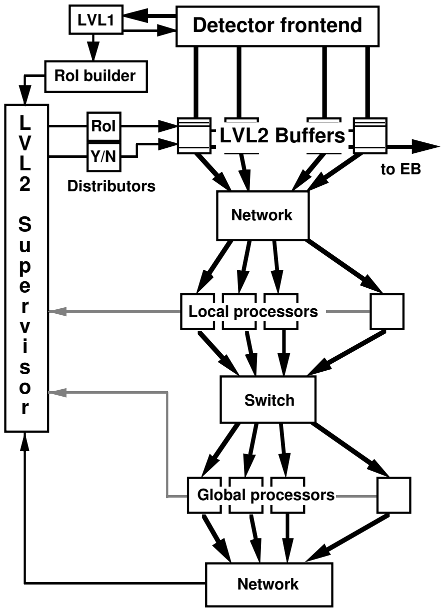

Figure 1.12: Architecture of the Level 2 trigger.

network to a set of local processors. Each of them reconstructs tracks in its RoI and passes the information generated to the global processors which collect data from all ROIs and make the final Level 2 decision. If it is negative, the event is simply flushed from the ROBs. If it is positive, the event is sent from the ROB's to the event builder (EB). The processing time of Level 2 is not fixed; on average it takes about 10 ms. The processors used here will be a farm of commercial platforms.

The data processed for each RoI by local processors at Level 2 includes:

- full ID information in the road given by the RoI,
- full granularity of EM and hadronic calorimeter information in a given RoI,
- muon system information for the RoI.

From this data we can obtain a good indication of particle type and energy that resulted in the acceptance of the event by the Level 2.

The global processors accumulate this information and match it to the Level 2 trigger menu (see Table 1.2). When a match is found, the Level 2 supervisor is notified to initiate event transfer to the EB together with the information built at the Level 2 stage. EB (or Level 2.5) collects this data and passes it to the Level 3.

1.4.4 The Level 3 trigger

The Level 3 is a farm of a multi-processor computing engines with full access to the EB and a permanent storage system. Its total input flow is 100–1000 MB/ s (100–1000 full events per second) and the average processing time is 1 s. The standard off-line detector reconstruction and track searching software is used to perform a full event reconstruction, as well as a detailed calculation of the missing transverse energy ($\not{E}_T$).

Additional selections decrease the output rate for one order of magnitude bringing us to an output flow of 10–100 MB/ s (10–100 events per second). The menus of the Level 3

Trigger	Rate [Hz]
Muon, $p_T > 40\,\mathrm{GeV}$	25
Isolated muon, $p_T > 20\,\mathrm{GeV}$	20
Two isolated muons, $p_T > 20\,\mathrm{GeV}$	5
Muon, $p_T > 20\,\mathrm{GeV} \oplus$ three jets, $p_T > 15\,\mathrm{GeV}$	50
Isolated muon, $p_T > 15\,\mathrm{GeV} \oplus$ isolated electron, $p_T > 15\,\mathrm{GeV}$	1
Two isolated muons, $p_T > 6\,\mathrm{GeV}$	10
Two isolated electrons, $p_T > 15\,\mathrm{GeV}$	8
Isolated muon, $p_T > 6\,\mathrm{GeV} \oplus$ two jets $p_T > 15\,\mathrm{GeV}$	200
Electron, $p_T > 80\,\mathrm{GeV}$	20
Isolated electron, $p_T > 20\,\mathrm{GeV}$	200
Isolated photon, $p_T > 40\,\mathrm{GeV}$	60
Two isolated photons, $p_T > 20\,\mathrm{GeV}$	5
Tau, $p_T > 150\,\mathrm{GeV}$	200
Two isolated taus, $p_T > 100\,\mathrm{GeV}$	5
Jet, $p_T > 500\,\mathrm{GeV}$	1
Two jets, $p_T > 400\,\mathrm{GeV}$	1
Two jets, $p_T > 100\,\mathrm{GeV} \oplus$ missing energy, $E_T > 100\,\mathrm{GeV}$	80
Four jets, $p_T > 100\,\mathrm{GeV}$	2
Jet, $p_T > 100\,\mathrm{GeV} \oplus$ three jets, $p_T > 15\,\mathrm{GeV}$	500
Four jets, $p_T > 50\,\mathrm{GeV}$	200
Missing energy, $E_T > 150\,\mathrm{GeV}$	30
Rate for Level 2 (without B-physics)	1 623

Table 1.2: An example of the Level 2 trigger menu for the low luminosity.

trigger are complex since they fully specify the selection criteria together with some cuts on sets of trigger objects. It also does a detailed calculation of the missing transverse energy ($\not{E}_T$).

When all is done and if the event passes the selection criteria, it's written to the permanent storage system. The trigger has finished its job.

1.4.5 Thou shalt compute

This is only half of the story. Another burden of the LHC experiments will be storing the data in an accessible format and providing computational infrastructure to carry out the physics analysis. In previous CERN experiments all the data gathered were stored, processed and eventually reprocessed at CERN. The computing environment for the LHC collaborations can be best characterized by the data production rate ($\sim 1\,\mathrm{PB/year}$) and expected number of simultaneous analyses (~ 500). CERN will not be in a position (and has already refused) to provide the infrastructure for all this ... so different strategies will have to be employed.

Fortunately LHC experiments are not the only clients for a large scale distributed computing. In past few years a new concept of meta-computing on a large scale has emerged, first from scientific communities and later also from industry (it has been named `Grid`). It is slightly unclear at present time how requirements for giga networks will be met in the future but due to a rapid expansion of the networking infrastructure one can expect them to be provided in a few coming years.

The plan of attack is to create several `regional centers` providing the CPU power for analysis and simulation, storage devices (in order of 100TB of permanent storage per year of running and approximately half of that amount of disk storage) and network bandwidth (1Mbps per active user and 100Mbps connection to CERN). For the successful management of these resources events and data must be efficiently tagged in order to provide access for analysis programs. Further description can be found in [13].

1.5 Role of electrons in the ATLAS physics programme

As with any species of detectable particle in any experiment, its role in a particular decay channel can be twofold. Firstly, it can be part of the decay products and the reconstruction efficiency and precision therefore directly influences the ability of measurements in the channel. Secondly, it can form a part of the background, the reconstruction of which can result in efficient background rejection.

In what follows an indication on the processes where electrons play a major role is given. A complete description of these processes can be found in 'ATLAS Detector and Physics performance TDR, volume II' [3].

1.5.1 Physics of the electro–weak gauge bosons

Gauge bosons and gauge boson pairs will be abundantly produced at the LHC. The large statistics and a high cms energy will allow several precision measurements to be carried out, which should improve significantly the precision achieved at present machines. Furthermore, their decay modes with electrons in the final state will be used to determine the mass scale of the EM calorimeter.

W mass

The W mass is one of the fundamental parameters of the Standard Model and is related to other parameters of the theory. Its uncertainty therefore influences other measurements by introducing errors on theoretical calculations.

The cross-section for the production of $pp \to \mathrm{W} + X;\ \mathrm{W} \to l\nu$ with $l = e, \mu$ is $\sigma(\mathrm{W}) \doteq 30\,\mathrm{nb}$ giving approximately 300 million events in one year of data taking at the low luminosity. Half of those are electron events.

The W mass measurement at hadron colliders is performed in the leptonic channels. Since the longitudinal momentum of the neutrino cannot be measured, the transverse mass m_T^{W} is used. Transverse momentum of the neutrino p_T^{ν} is obtained from the transverse momentum of the lepton p_T^{l} and that of the recoiling system u_T:

$$m_T^{\mathrm{W}} = \sqrt{2p_T^l p_T^\nu (1 - \cos\Delta\phi)}, \tag{1.1}$$

$$\vec{p}_T^{\,\nu} = -\vec{u}_T - \vec{p}_T^{\,l}, \tag{1.2}$$

where $\Delta\phi$ is the opening angle between the electron and the neutrino in the transverse plane.

The distribution of the m_T^{W} is sensitive to the W mass which can therefore be obtained by fitting experimental distribution to the Monte-Carlo samples generated with different values of m_{W}.

Gauge boson pair production

The non-abelian gauge-group structure of the electro-weak interactions predicts very specific couplings between the gauge bosons. They are referred to as Triple Gauge Couplings (TGC) and Quadruple Gauge Couplings (QGC). Any theory predicting physics beyond the SM can introduce deviations to these couplings. Precise measurements of the T/QGCs therefore provide not only a test of the SM but also a probe of a new physics in the gauge boson sector.

On ATLAS the TGCs will be observed in the leptonic decay modes of the Wγ and WZ production. In both cases electrons in the final state represent one half of the expected sample.

1.5.2 B–physics

ATLAS will perform most of the B physics at the low luminosity running while some of the studies can be pursued further also at the high luminosity operation (most of it limited by the b-layer lifetime). The mean value of the B hadron transverse momentum in observable channels is 16 GeV or more. The Level 1 trigger for B physics will be an inclusive muon trigger with $p_T \geq 6\,\mathrm{GeV}$ and $|\eta| < 2.4$. At Level 2 ATLAS will further trigger on the leptonic J/Ψ decays and $B^0 \to \pi^+\pi^-$.

As the $J/\Psi \to ee$ decays will be one of the entry points into the B physics, the quality of the electron reconstruction algorithms directly influences the trigger rates. Further, it enters into the analysis of the CP violation studies where the angle β of the unitary triangle is measured via the $B_d^0 \to J/\Psi K_s^0$ channel. For B_s^0 the angle γ, the width difference $\Delta\Gamma_s$ and mixing parameter $x_s = \Delta m_s/\Gamma_s$ will be observed via $B_s^0 \to J/\Psi\phi$.

Another important use of the $J/\Psi \to ee$ decay channel, although more technical in nature, is the calibration of the EM calorimeter at low energies.

1.5.3 Heavy quarks and leptons

Top quark physics

With the predicted production cross-section of $\sigma(t\bar{t}) = 833\,\mathrm{pb}$, the LHC will produce 8 million $t\bar{t}$ pairs per year of running at the low luminosity. Accurate measurement of m_t will improve the errors on theoretical calculations as well as help to constrain the SM Higgs boson mass. In the SM top quarks decay almost exclusively as $t \to \mathrm{W}b$. In 65.5% of all the events both W bosons will decay via $\mathrm{W} \to jj$ or at least one W will decay via $\mathrm{W} \to \tau\nu$. These events are hard to extract cleanly from the large multi-jet background and are not considered in ATLAS plans for the top physics. Instead at least one W is required to decay leptonically to either an electron or a muon. An energetic lepton with a large $\not{E}_T$ provides a clean trigger signature and a large suppression of the multi-jet background.

Fourth generation quarks and leptons

The data from LEP and the Tevatron imply the existence of only three SM families with light neutrinos. Models with heavy neutrinos have been proposed and current experimental limits on the fourth generation quarks and leptons are $m_Q > 128\,\mathrm{GeV}$ and $m_l > 80\,\mathrm{GeV}$. Fourth generation up-like quarks would predominantly decay via $u_4 \to \mathrm{W}b$ giving the same signature

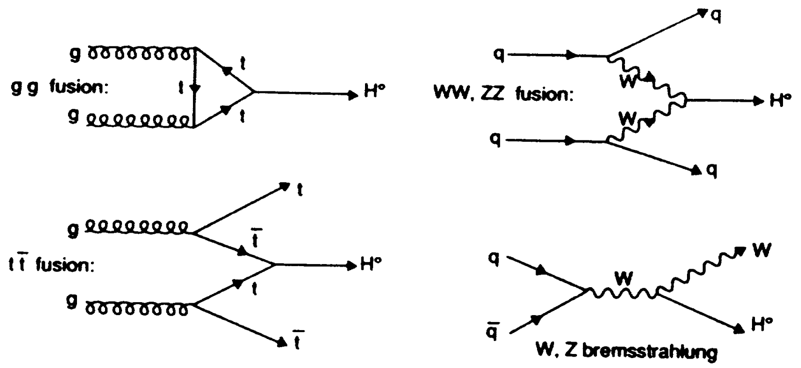

Figure 1.13: Feynmann diagrams representing major contributions to Higgs production cross–section in pp collisions.

as the top quark. Again, at least one of the Ws will be required to decay leptonically. For down-like quarks the dominant decay mode would be $d_4 \rightarrow tW$. For $pp \rightarrow d_4\bar{d}_4 \rightarrow t\bar{t}\mathrm{W}^+\mathrm{W}^- \rightarrow \mathrm{W}^+b\mathrm{W}^-\bar{b}\mathrm{W}^+\mathrm{W}^-$ at least one of the Ws is required to decay into leptons.

For heavy leptons $L \rightarrow N\mathrm{W}$ (N is the heavy neutrino) has been studied in some detail but it is not entirely clear whether this process could be separated from the background of single and pair productions of the W and Z bosons.

1.5.4 Standard Model Higgs boson searches

The experimental observation of one or several Higgs bosons will be fundamental to a better understanding of the electro-weak symmetry breaking. Its discovery and spectroscopy is one of the main physics goals of the ATLAS experiment. The detector is designed to observe it over a mass range from 80 GeV to 1 TeV in a variety of decay channels, the choice of which is given by the signal rates and signal to background ratios in various mass regions.

The main production channels of the Higgs boson at the LHC are shown in Fig.1.13. As associated Higgs production (H$t\bar{t}$, HW and HZ) is considered in all decay channels of interest and at least one lepton in final state is required by the trigger, efficient and accurate electron reconstruction is necessary for the analysis of the Higgs boson properties.

H $\rightarrow \gamma\gamma$

The decay mode H $\rightarrow \gamma\gamma$ is a rare decay mode, only observable over a limited Higgs boson mass range $80 < m_H < 150$ GeV. The biggest problem for an efficient reconstruction is resonant background from Z $\rightarrow ee$ decays which has a production cross-section roughly 25 000 times larger than the signal. To reduce this background below the 10% level, a rejection of ~ 500 per electron is required by the inner detector track reconstruction.

H $\rightarrow$ ZZ$^{(*)}$ and H $\rightarrow$ WW$^{(*)}$

H $\rightarrow$ ZZ* $\rightarrow 4l$ provides a clean signature in the Higgs boson mass range from 120 GeV to $2m_Z$. The branching ratio increases with m_H up to $m_H \sim 150$ GeV, where the H $\rightarrow$ WW channel begins to open up. Again, decay into leptons is favoured (WW$^{(*)} \rightarrow l\nu l\nu$) due to the abundant jet background at the LHC. In WW$^{(*)}$ it is not possible to directly reconstruct the Higgs boson mass peak. Instead one has to rely on properties of the distribution of reconstructed transverse mass [14].

In the case of $m_H > 2m_Z$ and up to 700 GeV, $\mathrm{H} \to ZZ \to 4l$ is the most reliable channel for the discovery. For a larger m_H its width becomes the limiting factor as the observed rates drop significantly. Only in this case the decay channels with jets in final states are also considered.

The mass resolution in the decay channels including electrons is dominated by the EM calorimeter precision and therefore depends crucially on the calorimeter calibration.